

## Binding of the ER $\alpha$ Nuclear Receptor to DNA Is Coupled to Proton Uptake<sup>†</sup>

Brian J. Deegan, Kenneth L. Seldeen, Caleb B. McDonald, Vikas Bhat, and Amjad Farooq\*

Department of Biochemistry and Molecular Biology and USylvester Braman Family Breast Cancer Institute,  
Leonard Miller School of Medicine, University of Miami, Miami, Florida 33136

Received March 23, 2010; Revised Manuscript Received May 24, 2010

**ABSTRACT:** Nuclear receptors act as ligand-modulated transcription factors and orchestrate a plethora of cellular functions central to health and disease. Although studied for more than half a century, many mysteries surrounding the mechanism of action of nuclear receptors remain unresolved. Herein, using isothermal titration calorimetry (ITC) in conjunction with macromolecular modeling (MM), we provide evidence that the binding of the ER $\alpha$  nuclear receptor to its DNA response element is coupled to proton uptake by two ionizable residues, H196 and E203, located at the protein–DNA interface. Alanine substitution of these ionizable residues decouples protonation and hampers the binding of ER $\alpha$  to DNA by nearly 1 order of magnitude. Remarkably, H196 and E203 are predominantly conserved across ~50 members of the nuclear receptor family, implying that proton-coupled equilibrium may serve as a key regulatory switch for modulating protein–DNA interactions central to nuclear receptor function and regulation. Taken together, our findings unearth an unexpected but critical step in the molecular action of nuclear receptors and suggest that they may act as sensors of intracellular pH.

Estrogen receptor  $\alpha$  (ER $\alpha$ )<sup>1</sup> is a member of a family of ligand-modulated transcription factors that have come to be known as nuclear receptors (NRs) (1–4). All members of NR family are evolutionarily related and share a core modular architecture comprised of a central DNA-binding (DB) domain flanked between an N-terminal transactivation (TA) domain and a C-terminal ligand-binding (LB) domain (5–7). A typical scenario for the activation of nuclear receptors involves the secretion of lipophilic messengers such as hormones and vitamins by appropriate tissues. Upon their diffusion through the cell membrane, these ligands bind to the LB domain of nuclear receptors and allow their translocation into the nucleus to modulate gene expression (8–10). While the DB domain recognizes specific promoter elements, the LB domain additionally serves as a platform for the recruitment of a multitude of cellular proteins, such as transcription factors, coactivators, and corepressors, to the site of DNA transcription, thereby allowing nuclear receptors to exert their action at the genomic level in a concerted fashion (11, 12). The TA domain is believed to be responsive to growth factors acting through the MAPK signaling and may further synergize the action of various coactivators and corepressors recruited by the LB domain at the site of DNA

transcription (13, 14). In this manner, nuclear receptors orchestrate a diverse array of cellular functions from embryonic development to metabolic homeostasis, and their malfunction has been widely implicated in disease (5, 15–19).

Discovered more than half a century ago, ER $\alpha$  mediates the action of estrogens such as estradiol, and its hyperactivation leads to the genesis of large fractions of breast cancer (20–26). The DB domain of ER $\alpha$  binds as a homodimer to the AGGTCA $n$ nT-GACCT consensus motif, termed the estrogen response element (ERE), located within the promoters of target genes (27). DNA binding is accomplished through a pair of tandem C4-type zinc fingers, with each finger containing a Zn<sup>2+</sup> ion coordinated in a tetrahedral arrangement by four highly conserved cysteine residues (28, 29). The first zinc finger (ZF-I) within each monomer of DB domain recognizes the hexanucleotide sequence 5'-AGGTCA-3' within the major groove at each end of the ERE duplex, while the second zinc finger (ZF-II) is responsible for the homodimerization of the DB domain upon DNA binding. Close scrutiny of the three-dimensional structure of the DB domain of ER $\alpha$  in complex with the ERE duplex reveals that a triplet of ionizable residues (D190, H196, and E203) either protrudes deep into the comfort of the major groove at the protein–DNA interface or appears to reside within touching distance of the DNA backbone (28) (Figure 1). Given that the placement of these residues in the proximity of the negatively charged phosphate backbone of DNA would be energetically unfavorable because of electrostatic repulsions, we hypothesized that the side chain moieties of D190, H196, and E203 may become protonated upon the binding of ER $\alpha$  to DNA to neutralize the intermolecular repulsions and further enhance the favorable role of electrostatic forces central to driving protein–DNA interactions. This notion is further corroborated by the fact that the imidazole side chain of H196 stacks against the highly basic side chain of K206, a scenario that could reduce the side chain pK<sub>a</sub> of H196 and thereby render it more amenable to protonation upon the

<sup>†</sup>This work was supported by the National Institutes of Health (Grant R01-GM083897) and the USylvester Braman Family Breast Cancer Institute (A.F.). C.B.M. is a recipient of a postdoctoral fellowship from the National Institutes of Health (T32-CA119929). B.J.D. and A.F. are members of the Sheila and David Fuente Graduate Program in Cancer Biology at the Sylvester Comprehensive Cancer Center of the University of Miami.

\*To whom correspondence should be addressed. E-mail: amjad@farooqlab.net. Phone: (305) 243-2429. Fax: (305) 243-3955.

Abbreviations: DB, DNA-binding; ER $\alpha$ , estrogen receptor  $\alpha$ ; ERE, estrogen response element; ITC, isothermal titration calorimetry; LB, ligand-binding; MALDI-TOF, matrix-assisted laser desorption ionization time-of-flight; MAPK, mitogen-activated protein kinase; NMR, nuclear magnetic resonance; NR, nuclear receptor; SEC, size-exclusion chromatography; TA, transactivation; Trx, thioredoxin; ZF, zinc finger.

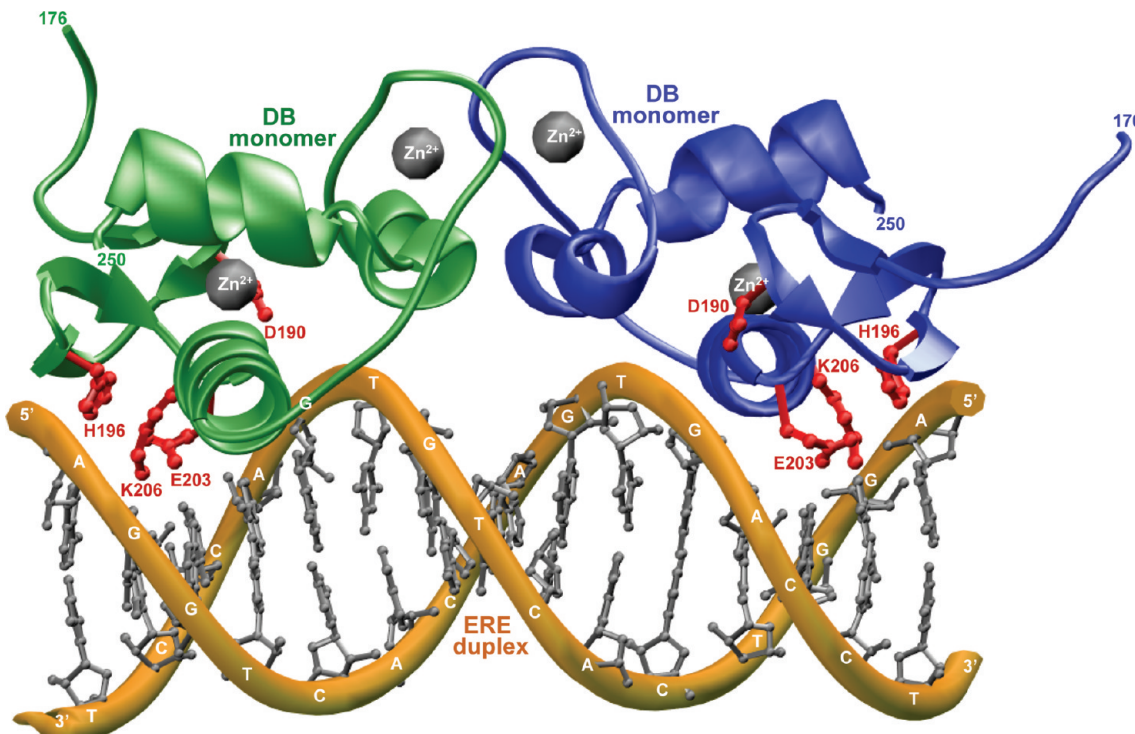


FIGURE 1: Three-dimensional atomic model of the DB domain of human ER $\alpha$  in complex with the ERE duplex containing the AGGTCA-cagTGACCT consensus sequence. Note that the DB domain binds to DNA as a homodimer. One monomer of the DB domain is colored green and the other blue. The Zn $^{2+}$  divalent ions are depicted as gray spheres, and the side chain moieties of D190, H196, E203, and K206 within the DB monomers are colored red. The DNA backbone is colored yellow, and the bases are colored gray for the sake of clarity. The numerals at the termini of DB monomers indicate the boundaries of the DB domain within the amino acid sequence of human ER $\alpha$ .

binding of the DB domain to DNA. It is also of note that the acidic side chains of D190 and E203 are positioned in the proximity of each other within the DB domain. It is thus conceivable that the more acidic side chain of D190 may be able to increase the pK<sub>a</sub> value of the side chain of E203, allowing it to become protonated more easily upon the binding of the DB domain to DNA at its own expense. Although both D190 and E203 are located at the protein–DNA interface, protonation of E203 would be more desirable as it directly inserts into the major groove of DNA.

In an effort to test our hypothesis, we have employed here isothermal titration calorimetry (ITC) in conjunction with macromolecular modeling (MM) to analyze the binding of the DB domain of ER $\alpha$  to a 21-mer dsDNA oligo containing the ERE motif, hereafter termed the ERE duplex. Our data reveal that H196 and E203, but not D190, indeed become protonated upon the binding of ER $\alpha$  to DNA. Furthermore, alanine substitution of these ionizable residues decouples protonation and hampers the binding of ER $\alpha$  to DNA by nearly 1 order of magnitude. Our study suggests that the proton-coupled equilibrium observed here may be a general feature of the nuclear receptor family.

## MATERIALS AND METHODS

**Protein Preparation.** The DB domain (residues 176–250) of human ER $\alpha$  (ExPasy entry P03372) was cloned into the pET102 bacterial expression vector, with an N-terminal thioredoxin (Trx) tag and a C-terminal polyhistidine (His) tag, using Invitrogen TOPO technology. The Trx tag was included to maximize protein expression in the soluble fraction, while the His tag was added to aid in protein purification through Ni-NTA affinity chromatography. Additionally, thrombin protease sites were introduced at

both the N- and C-termini of the DB domain to aid in the removal of tags after purification. The protein was subsequently expressed in the *Escherichia coli* BL21\*(DE3) bacterial strain (Invitrogen) and purified on a Ni-NTA affinity column using standard procedures. Briefly, bacterial cells were grown at 20 °C in LB medium supplemented with 50  $\mu$ M ZnCl<sub>2</sub> to an optical density of 0.5 at 600 nm prior to induction with 0.5 mM isopropyl  $\beta$ -D-thiogalactopyranoside (IPTG). The bacterial culture was further grown overnight at 20 °C, and the cells were subsequently harvested and disrupted using a BeadBeater (Biospec). After separation of cell debris via high-speed centrifugation, the cell lysate was loaded onto a Ni-NTA column and washed extensively with 20 mM imidazole to eliminate nonspecific binding of bacterial proteins to the column. The recombinant protein was subsequently eluted with 200 mM imidazole and dialyzed against an appropriate buffer to remove excess imidazole. Further treatment on a Hiload Superdex 200 size-exclusion chromatography (SEC) column coupled in-line with a GE Akta FPLC system led to purification of the recombinant DB domain to apparent homogeneity as judged by SDS-PAGE analysis. The identity of the recombinant protein was confirmed by MALDI-TOF mass spectrometry analysis. The final yield was typically between 5 and 10 mg of protein of apparent homogeneity per liter of bacterial culture. Treatment with thrombin protease significantly destabilized the recombinant DB domain, and it appeared to be proteolytically unstable. For this reason, except for control experiments to ensure that the tags had no effect on the binding of the DB domain to DNA, all experiments reported herein were conducted with the recombinant fusion DB domain containing a Trx tag at the N-terminus and a His tag at the C-terminus. The protein concentration was determined by the fluorescence-based Quant-It assay (Invitrogen) and spectrophotometrically using an extinction

coefficient of  $29045 \text{ M}^{-1} \text{ cm}^{-1}$  calculated for the recombinant fusion DB domain using the online software ProtParam at ExPasy Server (30). Results from both methods were in an excellent agreement.

**Site-Directed Mutagenesis.** The pET102 bacterial expression vector expressing the wild-type DB domain of ER $\alpha$  was subjected to the QuikChange Lightening kit (Stratagene) to generate single mutants D190A (DB\_D190A), S193A (DB\_S193A), H196A (DB\_H196A), Y197A (DB\_Y197A), S201A (DB\_S201A), E203A (DB\_E203A), K206A (DB\_K206A), K210A (DB\_K210A), and R211A (DB\_R211A) and double mutant H196A/E203A (DB\_AA). All mutant DB domains were expressed, purified, and characterized as described above. When analyzed by size-exclusion chromatography (SEC) using a Hiload Superdex 200 column, all mutant DB domains exhibited elution volumes virtually indistinguishable from those observed for the wild-type DB domain, implying that the point substitution of specific residues did not lead to protein unfolding and that the mutant DB domains retained the compact globular fold characteristic of the wild-type DB domain. These observations were further confirmed by circular dichroism (CD) analysis.

**DNA Synthesis.** 21-mer DNA oligos containing the ERE consensus site (AGGTCAnnnTGACCT) were commercially obtained from Sigma Genosys. The complete nucleotide sequences of the sense and antisense oligos constituting the ERE duplex were as follows:



Oligo concentrations were determined spectrophotometrically on the basis of their extinction coefficients derived from their nucleotide sequences using the online software OligoAnalyzer 3.0 (Integrated DNA Technologies) based on the nearest-neighbor model (31). To obtain double-stranded DNA (dsDNA) annealed oligos to generate the ERE duplex, equimolar amounts of sense and antisense oligos were mixed together and heated at 95 °C for 10 min and then allowed to cool to room temperature. The efficiency of oligo annealing to generate dsDNA was close to 100% as judged by Native-PAGE and circular dichroism (CD) analysis.

**ITC Measurements.** Isothermal titration calorimetry (ITC) experiments were performed on a Microcal VP-ITC instrument, and data were acquired and processed using fully automated features in Microcal ORIGIN. Measurements were repeated three or four times in phosphate, Hepes, Tricine, or Tris buffer. All buffers were taken to a final concentration of 50 mM containing 5 mM  $\beta$ -mercaptoethanol (pH 7.0). Additionally, 0–105 mM NaCl was added to adjust the ionic strength of all buffers to 110 mM. This ionic strength was sufficiently high to prevent nonspecific binding of the DB domain of ER $\alpha$  to DNA yet sufficiently low to allow ITC analysis to be conducted with a high signal-to-noise ratio. Various constructs of the DB domain and the ERE duplex were prepared in an appropriate buffer and degassed using the ThermoVac accessory for 5 min. The experiments were initiated via injection of  $25 \times 10 \mu\text{L}$  aliquots of 50–100  $\mu\text{M}$  ERE duplex from the syringe into the calorimetric cell containing 1.8 mL of a 5–10  $\mu\text{M}$  DB domain solution at 25 °C. The change in thermal power as a function of each injection was automatically recorded using Microcal ORIGIN,

and the raw data were further processed to yield binding isotherms of heat release per injection as a function of the molar ratio of ERE duplex to dimer-equivalent DB domain. The heats of mixing and dilution were subtracted from the heat of binding per injection by conducting a control experiment in which the same buffer in the calorimetric cell was titrated against the ERE duplex in an identical manner. Control experiments with scrambled dsDNA oligos generated a thermal power similar to that obtained for the buffer alone, implying that there was no nonspecific binding of the DB domain to noncognate DNA. Experiments that aimed to examine the binding of the thrombin-cleaved DB domain to DNA gave results similar to those of experiments conducted with the recombinant fusion protein, implying that the tags had no effect on DNA binding. However, because of the poor stability and low yield of the thrombin-cleaved DB domain and particularly in the case of mutant DB domains, all experiments reported here were conducted with the recombinant fusion DB domain containing a Trx tag at the N-terminus and a His tag at the C-terminus. Additionally, titration of a protein construct containing thioredoxin with a C-terminal His tag (Trx-His) in the calorimetric cell with the ERE duplex in the syringe produced no observable signal, implying that the tags do not interact with the ERE duplex. In a similar manner, titration of wild-type or mutant DB domains in the calorimetric cell with the Trx-His construct in the syringe produced no observable signal, implying that the tags do not interact with any of the wild-type or mutant DB domains. To extract the observed affinity ( $K_{\text{obs}}$ ) and observed enthalpy ( $\Delta H_{\text{obs}}$ ), the binding isotherms were iteratively fit to the following built-in function by nonlinear least-squares regression analysis using integrated Microcal ORIGIN:

$$q(i) = (nVP\Delta H_{\text{obs}}/2)\{1 + L/nP + K_{\text{obs}}/nP - [(1+L/nP+K_{\text{obs}}/nP)^2 - 4L/nP]^{1/2}\} \quad (1)$$

where  $q(i)$  is the heat release (kilocalories per mole) for the  $i$ th injection,  $n$  is the binding stoichiometry,  $V$  is the effective volume of protein solution in the calorimetric cell (1.46 mL),  $P$  is the total dimer-equivalent concentration of the DB domain in the calorimetric cell (micromolar), and  $L$  is the concentration of ERE duplex added (micromolar). Equation 1 is derived from the binding of a ligand to a macromolecule using the law of mass action assuming a one-site model (32). The observed free energy of binding ( $\Delta G_{\text{obs}}$ ) was calculated from the relationship

$$\Delta G_{\text{obs}} = RT \ln K_{\text{obs}} \quad (2)$$

where  $R$  is the universal molar gas constant (1.99 cal mol<sup>-1</sup> K<sup>-1</sup>) and  $T$  is the absolute temperature (298 K). The observed entropic contribution ( $T\Delta S_{\text{obs}}$ ) to binding was calculated from the relationship

$$T\Delta S_{\text{obs}} = \Delta H_{\text{obs}} - \Delta G_{\text{obs}} \quad (3)$$

The net change in the number of protons ( $\Delta m$ ) absorbed or released per DB monomer upon binding to DNA and the intrinsic binding enthalpy ( $\Delta H_{\text{int}}$ ) due to direct protein–DNA interactions and protonation of ionizable moieties were calculated from the slope and  $y$ -intercept of  $\Delta H_{\text{obs}} - \Delta H_{\text{ion}}$  plots by linear fits of data to the equation

$$\Delta H_{\text{obs}} = 2\Delta m\Delta H_{\text{ion}} + \Delta H_{\text{int}} \quad (4)$$

where  $\Delta H_{\text{obs}}$  is the observed binding enthalpy and  $\Delta H_{\text{ion}}$  is the ionization enthalpy of each buffer. The  $\Delta H_{\text{ion}}$  values of various

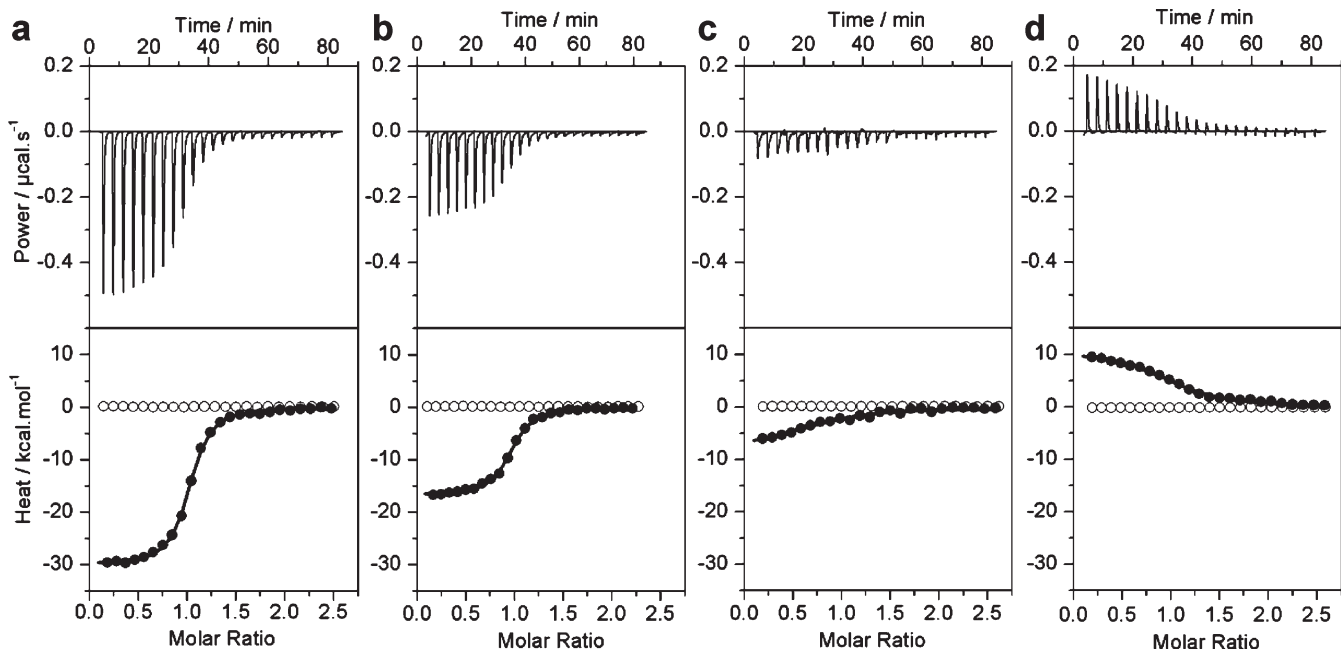


FIGURE 2: Representative ITC isotherms for the binding of the ERE duplex to the wild-type DB domain of ER $\alpha$  in phosphate (a), Hepes (b), Tricine (c), and Tris (d) buffers at pH 7.0 and 25 °C. The top panels show the raw ITC data expressed as the change in thermal power with respect to time over the period of titration. In the bottom panels, the change in molar heat is expressed as a function of the molar ratio of the ERE duplex to the dimer-equivalent DB domain (●). The solid lines in the bottom panels show the fit of data to a one-site model, as embodied in eq 1, using Microcal Origin. Note also that the DB domain shows no nonspecific binding to scrambled dsDNA oligos (○).

buffers were 1.22 kcal/mol for phosphate buffer, 5.02 kcal/mol for Hepes buffer, 7.64 kcal/mol for Tricine buffer, and 11.35 kcal/mol for Tris buffer (33–35).

**Macromolecular Modeling.** Macromolecular modeling (MM) was employed to generate a three-dimensional atomic model of the DB domain of ER $\alpha$  in complex with the ERE duplex using MODELER based on homology modeling (36). The X-ray structure of the DB domain of ER $\alpha$  in complex with a dsDNA oligo containing the ERE motif but with varying flanking sequences was used as a template (Protein Data Bank entry 1HCQ). A total of 100 atomic models were calculated, and the structure with the lowest energy, as judged by the MODELER Objective Function, was selected for further analysis. The atomic model was rendered using RIBBONS (37), and the electrostatic surface potentials were generated using MOLMOL (38).

## RESULTS AND DISCUSSION

**Binding of the DB Domain of ER $\alpha$  to DNA Is Coupled to Proton Uptake.** To test our hypothesis that the binding of ER $\alpha$  to DNA is coupled to proton uptake, we measured the binding of the DB domain of ER $\alpha$  to the ERE duplex in buffers of varying ionization enthalpies using ITC. Figure 2 shows representative ITC isotherms obtained from such measurements, while detailed thermodynamic parameters are listed in Table 1. It should be noted here that a classical test for ligand binding coupled to proton exchange is the dependence of the observed enthalpy ( $\Delta H_{\text{obs}}$ ) on ionization enthalpy ( $\Delta H_{\text{ion}}$ ) of the reaction buffer. Because different buffers are characterized by distinct ionization enthalpies, the observed enthalpy of ligand binding displays a sharp dependence on the buffer employed due to varying contributions from coupled protonation and deprotonation. Our data indeed suggest that the  $\Delta H_{\text{obs}}$  for the binding of the DB domain of ER $\alpha$  to DNA is highly dependent on the nature of buffer conditions employed (Figure 2). Thus, the  $\Delta H_{\text{obs}}$  of

binding goes from being highly exothermic (−30.52 kcal/mol) in phosphate buffer to being endothermic (9.82 kcal/mol) in Tris buffer and thereby mirrors the  $\Delta H_{\text{ion}}$  of the respective buffers ranging from 1.22 to 11.35 kcal/mol (33–35). This salient observation demonstrates that the binding of the DB domain of ER $\alpha$  to DNA is directly coupled to proton uptake. Although such a coupled equilibrium could result from the protonation of DNA bases, the side chain moieties of D190, H196, and E203 within the DB domain must be considered as the major suspects for proton uptake because of their proximity to the negatively charged phosphate backbone of DNA, a situation that would be inconceivable on thermodynamic grounds barring their protonation.

It is also worth noting that while the enthalpy is favorable for the binding of ER $\alpha$  to DNA in phosphate buffer, it contributes a substantial energetic penalty in Tris buffer (Table 1). In fact, close scrutinization of thermodynamic parameters observed for the binding of ER $\alpha$  to DNA in various buffers suggests that while enthalpy solely drives this protein–DNA interaction in phosphate and Hepes buffers of low ionization enthalpies, entropy plays a major role in Tris and Tricine buffers with high ionization enthalpies. In particular, in the case of Tris buffer, it is the entropy that drives binding against the backdrop of enthalpic penalty. These observations imply that physiological settings with low ionization enthalpies are likely to favor the binding of ER $\alpha$  to DNA, while the opposing conditions may be somewhat inhibitory. This is indeed corroborated by the fact that the binding affinity for formation of the ER $\alpha$ –DNA complex decreases by nearly 1 order of magnitude from 43 nM in phosphate buffer to 336 nM in Tris buffer (Table 1). It should be borne in mind that the favorable enthalpic contributions to binding largely result from the release of heat upon the formation of tight electrostatic interactions, hydrogen bonding, and hydrophobic contacts between protein and DNA. Thus, in buffers with low ionization enthalpies, the favorable enthalpic contribution is

Table 1: Observed Thermodynamic Parameters for the Binding of the ERE Duplex to the Wild-Type DB Domain of ER $\alpha$  in Various Buffers at pH 7.0 and 25 °C<sup>a</sup>

	$K_{\text{obs}}$ (nM)	$\Delta H_{\text{obs}}$ (kcal/mol)	$T\Delta S_{\text{obs}}$ (kcal/mol)	$\Delta G_{\text{obs}}$ (kcal/mol)
phosphate	43 ± 13	-30.52 ± 0.27	-20.44 ± 0.38	-10.08 ± 0.20
Hepes	59 ± 6	-17.22 ± 0.50	-7.34 ± 0.53	-9.88 ± 0.07
Tricine	238 ± 84	-6.06 ± 1.54	3.02 ± 1.68	-9.08 ± 0.23
Tris	336 ± 6	9.82 ± 0.64	19.10 ± 0.52	-8.94 ± 0.12

<sup>a</sup>The binding stoichiometries to the fits agreed within ±10%. Errors were calculated from three or four independent measurements. All errors are given to one standard deviation.

only slightly offset to compensate for the proton-coupled equilibrium, rendering enthalpy as the sole driving force accompanied by an entropic penalty. In contrast, in buffers with high ionization enthalpies, the favorable enthalpic contribution is largely offset and even overridden by the enthalpic penalty due to the proton-coupled equilibrium with entropy either contributing favorably or serving as the sole driving force at the expense of enthalpy.

This reciprocal relationship between enthalpy and entropy lies in the enthalpy–entropy compensation phenomenon (39–43); macromolecular interactions are compensated by equal but opposing entropic changes such that there is little or no net gain in the overall free energy. Thus, buffers with high ionization enthalpies gain a substantial increase in entropy upon the release of a proton, presumably due to an increase in the degrees of freedom that become available to water molecules after they are freed from their hydration shell surrounding the exchangeable proton prior to its release. However, in the case of buffers with low ionization enthalpies, the exchangeable proton would be expected to be more “economically” hydrated such that the release of water molecules from the rather small hydration shell contributes relatively little to the overall entropy gain but at the same time draws less heat to be removed. Such enthalpy–entropy compensations for the binding of the DB domain to the ERE duplex in various buffers are illustrated in Figure 3a. Consistent with the foregoing arguments, it should also be noted that while the increase in the binding affinity of the DB domain for DNA correlates with the overall favorable enthalpy change in various buffers, the increase in the favorable entropy change seems to oppose such protein–DNA interactions (Figure 3b,c).

**Residues H196 and E203 Serve as Sole Proton Acceptors upon the Binding of ER $\alpha$  to DNA.** For processes in which ligand binding is coupled to proton exchange, the observed enthalpy ( $\Delta H_{\text{obs}}$ ) is related to the ionization enthalpy ( $\Delta H_{\text{ion}}$ ) by the relationship  $\Delta H_{\text{obs}} = 2\Delta m\Delta H_{\text{ion}} + \Delta H_{\text{int}}$ , where  $\Delta m$  is the net change in the number of protons absorbed or released per DB monomer upon binding to DNA and  $\Delta H_{\text{int}}$  is the intrinsic binding enthalpy due to direct protein–DNA interactions and protonation of ionizable moieties. A plot of  $\Delta H_{\text{obs}}$  versus  $\Delta H_{\text{ion}}$  should thus yield a linear curve with the slope  $2\Delta m$  and y-intercept equal to  $\Delta H_{\text{int}}$ . As shown in Figure 4, such analysis reveals that the binding of the wild-type DB domain (DB\_WT) of ER $\alpha$  to DNA results in the uptake of two protons per DB monomer. It should be noted here that a positive slope equates to proton uptake and a negative slope to proton release in this analysis. The fact that the binding of each monomer of the DB domain to DNA is coupled to a net uptake of two protons implies that at least two of the three possible residues (D190, H196, and E203) may serve as proton acceptors. Could it be possible that only two

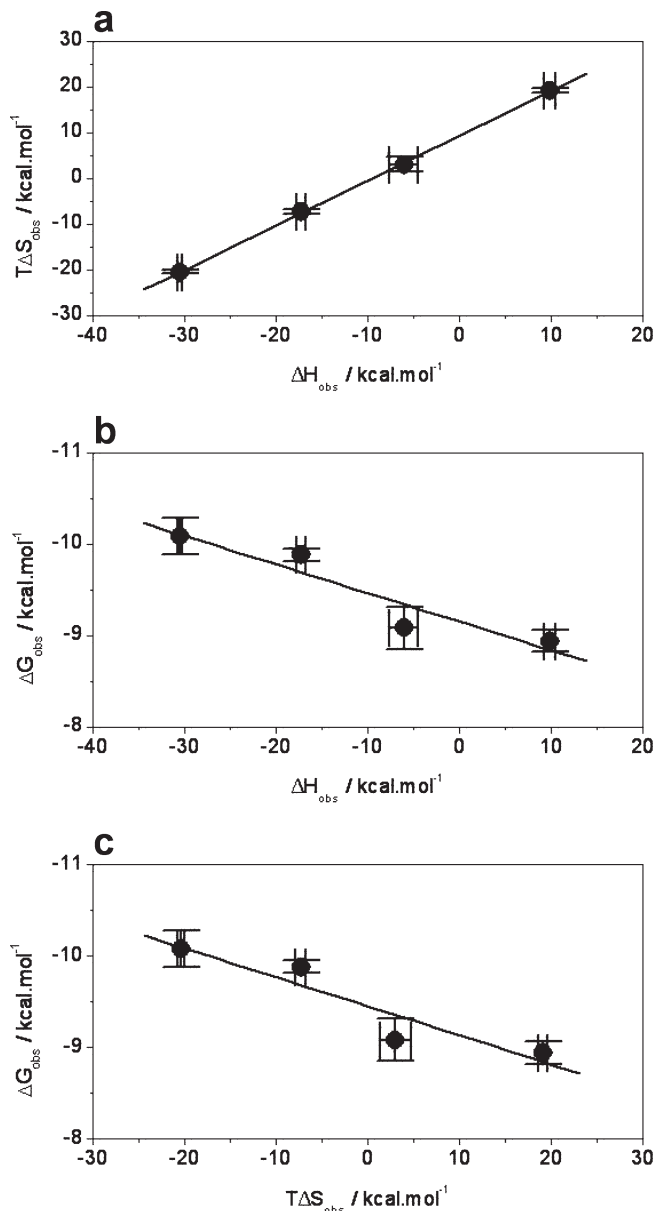


FIGURE 3: Interdependence of the observed enthalpic change ( $\Delta H_{\text{obs}}$ ), entropic change ( $T\Delta S_{\text{obs}}$ ), and free energy change ( $\Delta G_{\text{obs}}$ ) for the binding of the ERE duplex to the wild-type DB domain of ER $\alpha$  in various buffers: (a)  $\Delta H_{\text{obs}}$  –  $T\Delta S_{\text{obs}}$  plot, (b)  $\Delta H_{\text{obs}}$  –  $\Delta G_{\text{obs}}$  plot, and (c)  $T\Delta S_{\text{obs}}$  –  $\Delta G_{\text{obs}}$  plot. Note that the solid lines represent linear fits to the data in all plots. All error bars were calculated from three or four independent measurements and are given to one standard deviation.

of these residues are involved in proton uptake, or do all three residues fractionally contribute to a net uptake of two protons?

To address this question, we introduced single alanine substitutions at positions D190, H196, and E203 within the DB domain and then bound these mutant domains to the ERE duplex using ITC. The  $\Delta H_{\text{obs}}$  –  $\Delta H_{\text{ion}}$  plot for the binding of the D190A mutant of the DB domain (DB\_D190A) to DNA reveals that there is no net change in the number of protons exchanged relative to the DB\_WT domain (Figure 4), implying that D190 is most likely not responsible for the proton-coupled equilibrium observed here. In striking contrast, the  $\Delta H_{\text{obs}}$  –  $\Delta H_{\text{ion}}$  plots for the binding of H196A (DB\_H196A) and E203A (DB\_E203A) mutants of the DB domain to DNA reveal that only one proton is exchanged in each case (Figure 4), arguing strongly that residues H196 and E203 are the sole sites of protonation.

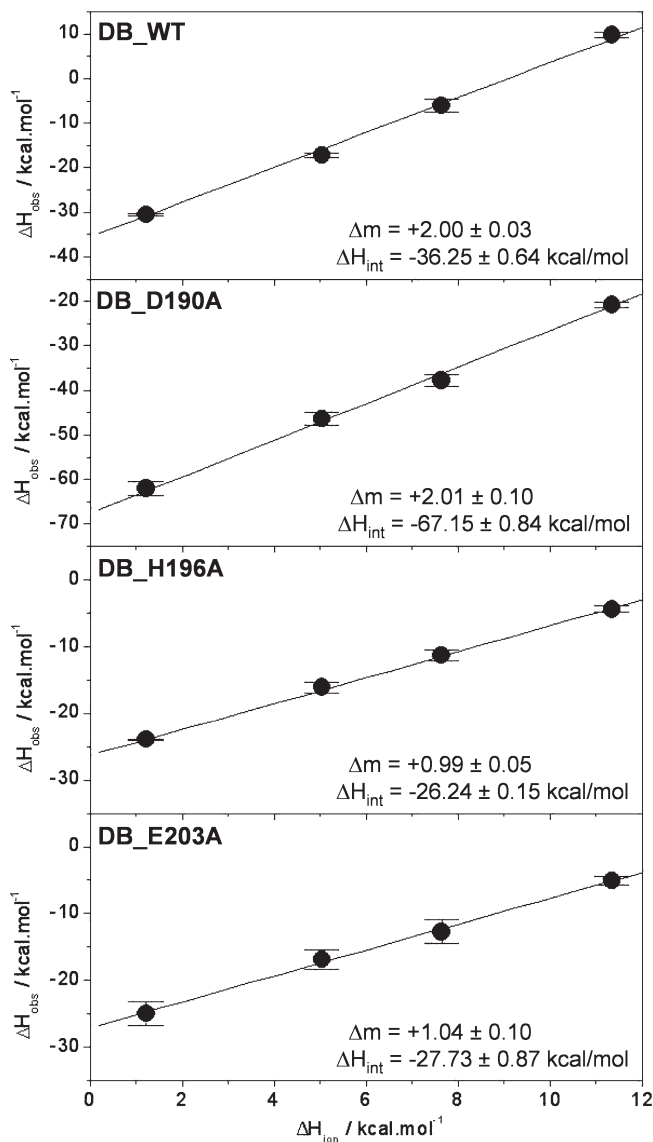


FIGURE 4: Dependence of the observed enthalpy ( $\Delta H_{\text{obs}}$ ) as a function of ionization enthalpy ( $\Delta H_{\text{ion}}$ ) of various buffers upon the binding of the ERE duplex to the wild-type DB domain (DB\_WT), the D190A single mutant of the DB domain (DB\_D190A), the H196A single mutant of the DB domain (DB\_H196A), and the E203A single mutant of the DB domain (DB\_E203A) of ER $\alpha$  at pH 7.0 and 25 °C. The  $\Delta H_{\text{ion}}$  values of various buffers used were 1.22 kcal/mol for phosphate buffer, 5.02 kcal/mol for Hepes buffer, 7.64 kcal/mol for Tricine buffer, and 11.35 kcal/mol for Tris buffer (33–35). The solid lines within each panel represent fits of data points to eq 4. Note that the net change in the number of protons ( $\Delta m$ ) absorbed or released per DB monomer upon binding to DNA and the intrinsic binding enthalpy ( $\Delta H_{\text{int}}$ ) due to direct protein–DNA interactions and protonation of ionizable moieties for each DB construct are provided within the corresponding panels. Error bars were calculated from three or four independent measurements. All errors are given to one standard deviation.

Table 2 provides complete thermodynamic parameters for the binding of wild-type and various mutants of the DB domain to the ERE duplex in phosphate buffer. It is clearly evident from these data that while the D190A mutation has little effect on the binding affinity of the DB domain for DNA, H196A and E203A mutations both reduce the binding affinity by severalfold. Remarkably, the binding of the H196A/E203A double mutant of the DB domain (DB\_AA) to DNA is ~1 order of magnitude weaker than that of the wild-type DB domain (DB\_WT), arguing

further that both H196 and E203 are likely involved in proton uptake upon the binding of ER $\alpha$  to DNA. It should, however, be noted that the poor stability of the DB\_AA construct made measurements feasible only in phosphate buffer, and no reliable analysis could be conducted in other buffers for direct comparison with the DB\_WT construct. It is also of interest that while the H196A and E203A mutations result in the reduction of enthalpy for the binding of the DB domain to DNA by ~5–7 kcal/mol due to removal of the enthalpic contribution of protonation at H196 or E203 and corresponding protein–DNA interactions at these positions, the enthalpy change for the D190A mutation is nearly 2-fold more favorable relative to the wild-type DB domain (Table 2). It is thus conceivable that the D190A mutation results in local secondary and tertiary structural changes within the DB domain and that the partial folding of the DB\_D190A mutant domain upon binding to DNA also favorably contributes to the binding enthalpy. However, such an enhancement in favorable enthalpy does not translate into a higher binding affinity of the D190A mutant domain for DNA due to an equally compensating entropic contribution as discussed in the previous section.

*pH Tightly Regulates the Binding of the DB Domain of ER $\alpha$  to DNA.* In an effort to further support the notion that the residues H196 and E203 serve as the sole sites of protonation upon the binding of ER $\alpha$  to DNA, we analyzed the binding of wild-type (DB\_WT) and double mutant H196A/E203A (DB\_AA) constructs of the DB domain to the ERE duplex as a function of solution pH (Figure 5). Our data reveal that while the binding affinity of the DB\_WT construct for DNA is sharply dependent on solution pH in a sigmoidal fashion, the binding affinity of the DB\_AA construct for DNA is independent of solution pH (Figure 5a). Taken collectively, our data suggest strongly that the binding of the DB domain of ER $\alpha$  is coupled to proton uptake and that the side chain moieties of H196 and E203 serve as sole proton acceptors in this capacity.

It is, however, noteworthy that the protonation of H196 and E203 within ER $\alpha$  could precede or follow the subsequent binding of DNA. In this manner, ER $\alpha$  could bind to DNA in both the protonated and unprotonated forms. Figure 6 provides a thermodynamic cycle for the various equilibria linked to the binding of ER $\alpha$  to DNA. It is clearly evident from such a cycle that the binding of ER $\alpha$  to DNA may or may not be coupled to proton uptake depending on solution pH. Thus, at low pH values, ER $\alpha$  may become fully protonated prior to binding DNA. On the other hand, at high pH values, ER $\alpha$  may become fully unprotonated and the proton uptake may be decoupled for its binding to DNA. The fact that ER $\alpha$  can bind to DNA both in the protonated form and in the unprotonated form is further supported by the sigmoidal response of the binding affinity ( $K_{\text{obs}}$ ) of DB\_WT for DNA as a function of pH (Figure 5a). Thus, the plateau values of the  $1/K_{\text{obs}}$ –pH plot at low and high pH values correspond to the intrinsic binding affinities of the protonated and unprotonated forms of DB\_WT domain for DNA, respectively.

It should also be noted that the  $\Delta H_{\text{obs}}$ –pH and  $T\Delta S_{\text{obs}}$ –pH plots for the binding of the DB\_WT domain to DNA display bell-shaped curves characteristic of a proton-coupled ligand binding event (Figure 5b, top and middle panels). Such behavior arises due to the fact that the enthalpy of protonation of the free form is different from that of the liganded form. Since the ratio of free and liganded forms of the protein varies as a function of pH in going from a low pH value to a high pH

Table 2: Observed Thermodynamic Parameters for the Binding of the ERE Duplex to Wild-Type and Various Mutant Constructs of the DB Domain of ER $\alpha$  in Phosphate Buffer at pH 7.0 and 25 °C<sup>a</sup>

	$K_{\text{obs}}$ (nM)	$\Delta H_{\text{obs}}$ (kcal/mol)	$T\Delta S_{\text{obs}}$ (kcal/mol)	$\Delta G_{\text{obs}}$ (kcal/mol)
DB_WT	43 ± 13	-30.52 ± 0.27	-20.44 ± 0.38	-10.08 ± 0.20
DB_D190A	67 ± 6	-62.05 ± 1.64	-52.33 ± 1.48	-9.80 ± 0.06
DB_H196A	190 ± 24	-23.95 ± 0.08	-14.76 ± 0.14	-9.18 ± 0.07
DB_E203A	172 ± 48	-24.97 ± 1.81	-15.66 ± 1.97	-9.26 ± 0.17
DB_AA	387 ± 90	-23.77 ± 2.29	-15.00 ± 2.36	-8.77 ± 0.14
DB_S193A	102 ± 10	-45.10 ± 1.29	-35.54 ± 1.25	-9.55 ± 0.04
DB_Y197A	316 ± 7	-31.12 ± 0.41	-22.24 ± 0.37	-8.88 ± 0.02
DB_S201A	119 ± 9	-28.70 ± 0.69	-19.23 ± 0.64	-9.46 ± 0.05
DB_K206A	313 ± 6	-30.86 ± 0.86	-21.97 ± 0.85	-8.89 ± 0.07
DB_K210A	326 ± 11	-25.96 ± 0.17	-17.09 ± 0.18	-8.86 ± 0.09
DB_R211A	745 ± 76	-8.21 ± 0.09	0.17 ± 0.10	-8.38 ± 0.11

<sup>a</sup>The various constructs of the DB domain are the wild-type construct (DB\_WT), the single mutant constructs (DB\_D190A, DB\_H196A, DB\_E203A, DB\_S193A, DB\_Y197A, DB\_S201A, DB\_K206A, DB\_K210A, and DB\_R211A), and the H196A/E203A double mutant construct (DB\_AA). The binding stoichiometries to the fits agreed within ±10%. Errors were calculated from three or four independent measurements. All errors are given to one standard deviation.

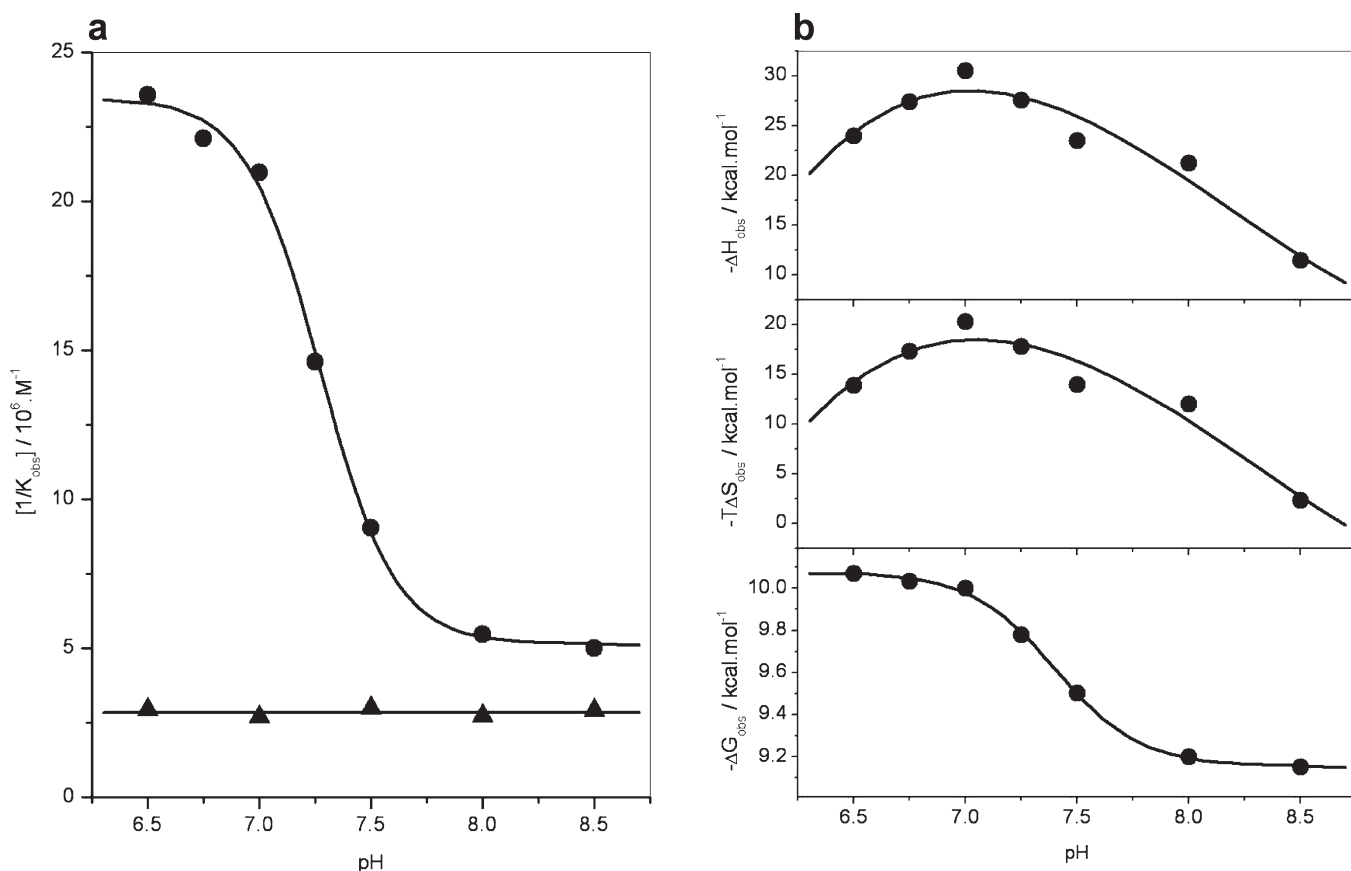


FIGURE 5: Dependence of thermodynamics on pH for the binding of the ERE duplex to the wild-type DB domain (DB\_WT) and the H196A/E203A double mutant of the DB domain (DB\_AA) of ER $\alpha$  in phosphate buffer at 25 °C. (a) Representative  $1/K_{\text{obs}}$ –pH plots for the DB\_WT (●) and DB\_AA (▲) domains. The solid lines indicate sigmoidal and linear fits to data points for the sake of clarity. (b) Representative  $\Delta H_{\text{obs}}$ –pH (top),  $T\Delta S_{\text{obs}}$ –pH (middle), and  $\Delta G_{\text{obs}}$ –pH (bottom) plots for the DB\_WT domain. In the top and middle panels, the solid lines indicate polynomial fits to data points for the sake of clarity. In the bottom panel, the solid line indicates a sigmoidal fit to data points for the sake of clarity.

value, the enthalpic contribution due to their protonation to the observed enthalpy varies accordingly, reaching zero at the extreme values and a maximum between these extremes where the ratio of the protonation of the free form to the liganded form equals unity. Expectedly, the  $\Delta G_{\text{obs}}$ –pH plot for the binding of DB\_WT to DNA follows sigmoidal behavior, in agreement with the ability of both the protonated and unprotonated forms to bind to DNA with distinct affinities (Figure 5b, bottom panel).

**Electrostatic Surface Potentials Reveal That the Protonation of H196 and E203 Optimizes Thermodynamic Constraints.** In an attempt to rationalize the effect of protonation of H196 and E203 on electrostatics at the protein–DNA interface, we generated molecular surfaces of the DB domain of ER $\alpha$  in complex with the ERE duplex depicting protein electrostatic potentials (Figure 7). Our data reveal how such protonation switches polarization of protein surface at residues H196 and E203 to render it thermodynamically more favorable for

coming into contact with DNA. In the free conformation, H196 and E203 occupy what appear to be neutral and negatively charged spots on the protein surface, respectively, that are destined to come into close contact with DNA. It is further evident that while the presence of neutral charge at H196 may not in any way compromise the subsequent binding of DNA, protonation at this position could bring about favorable energetic contributions as a direct result of favorable electrostatic interactions with the negatively charged phosphate backbone.

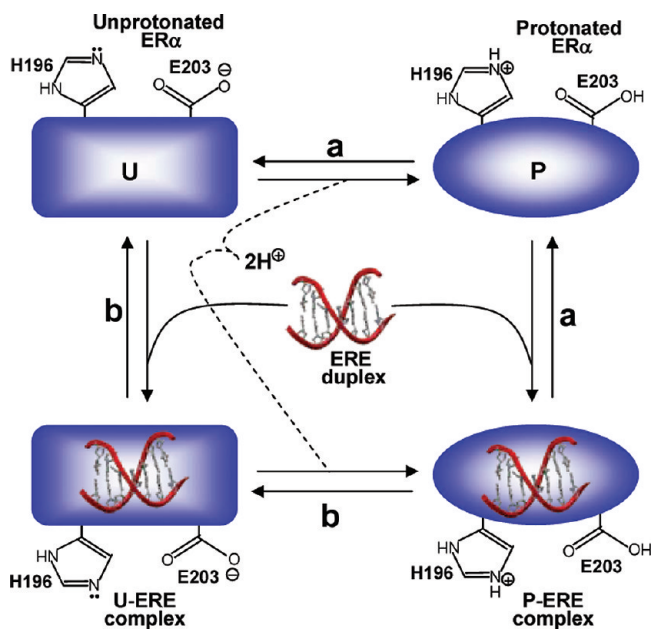


FIGURE 6: Thermodynamic cycle for the various equilibria linked to the binding of ER $\alpha$  to DNA. (a) ER $\alpha$  becomes protonated in the free form, and the resulting protonated form (P) binds to DNA. (b) ER $\alpha$  binds to DNA in the unprotonated form (U), and the resulting liganded form becomes protonated.

In contrast, the buildup of negative charge at E203 would hamper the subsequent binding of DNA due to electrostatic repulsions with the negatively charged phosphate backbone, suggesting that protonation at this position would relieve such energetic barriers. Taken together, the electrostatic surface potentials of the DB domain of ER $\alpha$  alone and in complex with DNA argue strongly that the protonation of H196 and E203 would optimize thermodynamic constraints to allow the two molecular surfaces to come into the proximity of one another to attain a tight molecular fit worthy of the rather high affinity that this DNA–protein complex displays.

**Proton-Coupled Binding to DNA Appears To Be a Hallmark of the Nuclear Receptor Family.** In an attempt to analyze the extent to which the ability of ER $\alpha$  to become protonated upon binding to DNA is shared by other members, we generated an amino acid sequence alignment of the DB domains of the entire human NR family (Figure 8). It should be noted that the DB domains of NR family are poorly conserved and are <15% identical in sequence outside the quartet of cysteine residues involved in coordinating the Zn $^{2+}$  divalent ion within each of the two zinc fingers of the DB domain. Thus, the residues conserved among the various DB domains bear a significant importance and must have coevolved for a common physiological function.

Remarkably, H196 and E203 rank among these conserved residues within the DB domains of the human NR family. Thus, while H196 is absolutely conserved within all members of the human NR family, E203 is predominantly conserved in most members, with notable exceptions being the androgen receptor (AR), glucocorticoid receptor (GR), mineralocorticoid receptor (MR), and progesterone receptor (PR), which all have a glycine substitution for E203. Interestingly, E203 is substituted with an asparagine in the photoreceptor-specific nuclear receptor (PNR), implying that hydrogen bonding at this position may play a critical role in protein–DNA interaction pertinent to the physiological function of this nuclear receptor. Finally, E203 is substituted with a related acidic and ionizable aspartate residue

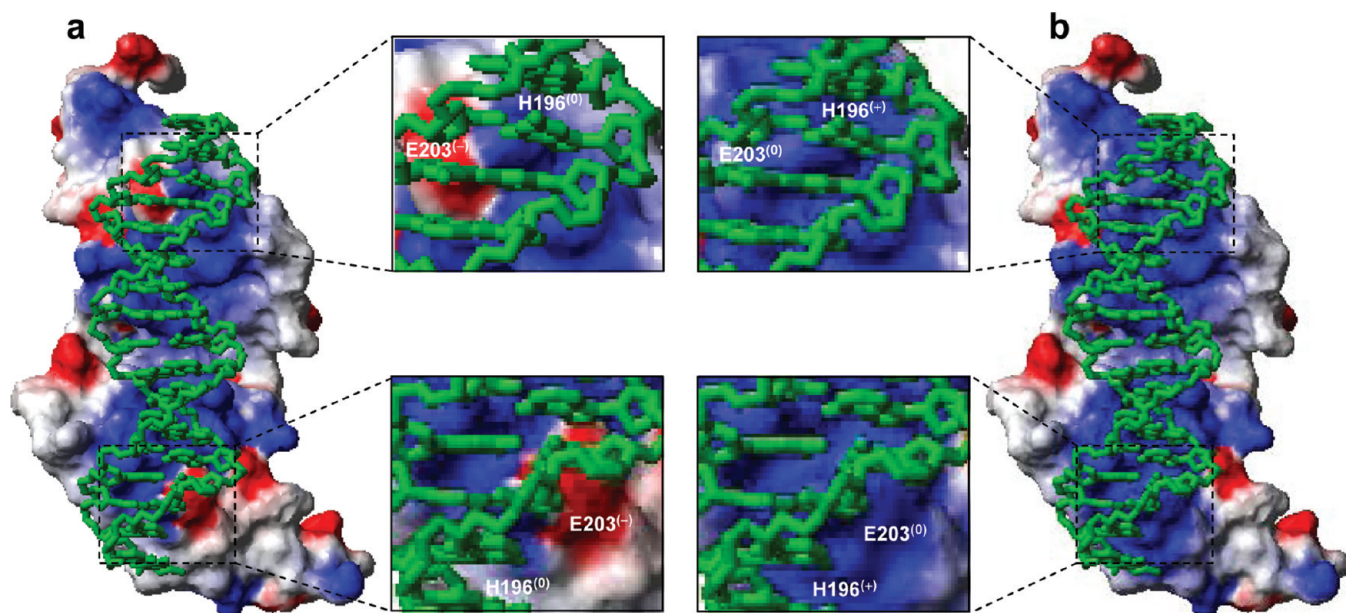


FIGURE 7: Molecular surfaces depicting electrostatic potentials of the DB domain of ER $\alpha$  containing H196 and E203 in unprotonated forms (a) and protonated forms (b) in complex with the ERE duplex. The blue and red colors denote the density of positive and negative charges, respectively, while the apolar and polar surfaces are indicated by white/gray color on the molecular surfaces. In the expanded views, the locations of H196 and E203 are clearly marked on the molecular surfaces, the parentheses indicating the overall charge on each residue under unprotonated and protonated forms. The ERE duplex is displayed as a stick model and colored green for the sake of clarity.

	ZF-I	ZF-II	
	D190 H196 E203 K206		
	* * * *	* * * *	
ER $\alpha$	176-MESAKETRYCAVCDYASGYHYGVWSCEGCKAFFKRSIQQ--HNDYMC--TNQCTIDKNRKRSCQACRLRKCYEVGM-250		P03372
ER $\beta$	140-PGSKRDAHFCAVCSDYASGYHYGVWSCEGCKAFFKRSIQQ--HNDYICPA--TNQCTIDKNRKRSCQACRLRKCYEVGM-214		Q92731
ERR $\alpha$	070-VLSSLPKRLCLVCGDVASGYHYGVASCEACKAFFKRTIQQ--SIEYSCPA--SNECEITKRRRKACQACRFTKCLRVGM-144		P11474
ERR $\beta$	094-MLNAPIPKRLCLVCGDIASGYHYGVASCEACKAFFKRTIQQ--NIEYSCPA--TNECEITKRRRKSCQACRFFMKCLKVGM-168		O95718
ERR $\gamma$	119-MLNSMPKRLCLVCGDIASGYHYGVASCEACKAFFKRTIQQ--NIEYSCPA--TNECEITKRRRKSCQACRFFMKCLKVGM-193		P62508
ARP1	070-KQQQQHIECVVCGDKSSGKHYGQFTCEGCKSFFKRSVRR--NLSYTCRA--NRNCPIDQHHRNQCQYCRLLKCKLVGM-144		P24468
CAR	002-ASREDELRCVVCGDQATGYHFNALTCEGCKGFFRTVSK--SIGPTCPF--AGSCEVSKTQRHCACRFFMKCLDAGM-076		Q14994
EAR2	047-EERPLGLQVDVVCGDKSSGKHYGFTCEGCKSFFKRSIIRR--NLSYTCRS--NRDCQIDQHHRNQCQYCRLLKCKFRVGM-121		P10588
EAR3	077-SGQQQHIECVVCGDKSSGKHYGQFTCEGCKSFFKRSVRR--NLTYTCRA--NRNCPIDQHHRNQCQYCRLLKCKLVGM-151		P10589
FXR	128-AGRIKGDELCVVCGDRASGYHYNALTECEGCKGFFRRSITK--NAVYKCKN--GGNCVMDMYMRKCQECLRKCKEMGM-202		Q96RI1
GCNF	051-SDDRAEQRCTLCICGDRATGLHYGIISCEGCKGFFKRSICN--KRVYCSR--DKNCVMSRQNRNCQYCRLLKCLQMG-125		Q15406
LRH1	077-SYDEELLECPVCGDKVSGHYGLLTCEGCKGFFKRTVQN--NKRYTCIE--NQNCQIDKTQRKRCYCRFQKCLSVGM-151		O00482
LX $\alpha$	089-APKMLGNELCSVCGDKASGFHYNVLSCEGCKGFFRRSVNV--GAHYICHS--GGHPMDTYMRKCQECLRKCRQAGM-163		Q13133
LX $\beta$	078-APKMLGHLCRVCGDKASGFHYNVLSCEGCKGFFRRSVVRGGARRYACRG--GGTCQMDAFMRKCQQCRLRKCKEAGM-154		P55055
NGFIB	257-GSSGGSEGRCAVCGDNASCQHYGVRTCEGCKGFFKRTVQK--SAKYICLA--NKDCPVDKRRRNRCQFCRFQKCLAVGM-331		P22829
NOR1	283-RSSSSSEGETCAVCGDNAACQHYGVRTCEGCKGFFKRTVQK--NAKYVCLA--NKNCPVDKRRRNRCQYCRFQKCLAVGM-357		Q92570
NURR1	254-RGSPSNEGLCAVCGDNAACQHYGVRTCEGCKGFFKRTVQK--NAKYVCLA--NKNCPVDKRRRNRCQYCRFQKCLAVGM-328		P43354
PPAR $\alpha$	093-SPSGALNIECRI CGDKASGYHYGVHACEGCKGFFRRTIRL-KLVDKCDR---SCKI QKKRNKCQYCRFHKCLSVGM-166		Q07869
PPAR $\beta$	065-ASCGSLNMECRVCGDKASGFHYGVHACEGCKGFFRRTIRM-KLEYEKCR---SCKI QKKRNKCQYCRFQKCLALGM-138		Q03181
PPAR $\gamma$	130-PSNSLMAIECRVCGDKASGFHYGVHACEGCKGFFRRTIRLKLHYDR-CDL---NCRIHKKSRNKCQYCRFQKCLAVGM-203		P37231
PXR	031-DEEVGGPQICRVCGDKATGYHFNVMTCEGCKGFFRRAK--RNARLRCPF-RKGACEITRKTRRQCAQCRLLRKCLESGM-107		O75469
RAR $\alpha$	079-PPLPRIYKPCFVQDKSSGYHYGVSACEGCKGFFRRSIQQ--KNMVYTCHR--DKNCIINKVTRRNRCQYCRLLRKCFEVGM-153		P10276
RAR $\beta$	079-LPPPRTVYKPCFVQDKSSGYHYGVSACEGCKGFFRRSIQQ--NMIVYTCR--DKNCVINKVTRRNRCQYCRLLRKCFEVGM-153		P10826
RAR $\gamma$	081-PPPPRTVYKPCFVQDKSSGYHYGVSSCEGCKGFFRRSIQQ--NMIVYTCR--DKNCIINKVTRRNRCQYCRLLRKCFEVGM-155		P13631
RE $\alpha$	123-TKLMGMVLLCKVCGDVASGFHYGVHACEGCKGFFRRSIQQ-NIQYKRCLK--NENCSIVRINRNRCQQCRCFKKCLSVGM-198		P20393
RE $\beta$	094-TKFSGMVLLCKVCGDVASGFHYGVHACEGCKGFFRRSIQQ-NIQYKRCLK--NENCSIMRMNRNRCQQCRCFKKCLSVGM-169		Q14995
ROR $\alpha$	097-MNAQIEIIPCKICGDKSSGIHYGVITCEGCKGFFRRSQQS--NATYSCPR--QKNCLIDRTSRNRCQHCRLLRKCLALGM-171		P35398
ROR $\beta$	012-ATAQIEVIPCKICGDKSSGIHYGVITCEGCKGFFRRSQSN--NASYSCPR--QRNCLIDRTNRNRCQHCRLLRKCLALGM-086		Q92753
ROR $\gamma$	022-HTSQIEVIPCKICGDKSSGIHYGVITCEGCKGFFRRSQRC--NAAYSCTR--QNCNCPIDRTSRNRCQHCRLLRKCLALGM-096		P51449
RX $\alpha$	126-NMASFTKHI $\text{CAI}$ CGDRSSGKHYGVYSCEGCKGFFKRTVTK--DLTYTCRD--NKDCCLIDKRQRNRCQYCRYQKCLAMGM-200		P19793
RX $\beta$	196-GGPGAGKRL $\text{CAI}$ CGDRSSGKHYGVYSCEGCKGFFKRTIRK--DLTYSCRD--NKDCVTDKQRNRCQYCRYQKCLATGM-270		P28702
RX $\gamma$	130-SPGSLVKH $\text{CAI}$ CGDRSSGKHYGVYSCEGCKGFFKRTIRK--DLIYTCDR--NKDCCLIDKRQRNRCQYCRYQKCLVMGM-204		P48443
SF1	004-SYDEDLDELCPVCGDKVSGHYGLLTCEGCKGFFRRTVQN--NKHYTC--SQSKICKDTQRKRCPFCRFQKCLTVGM-078		Q13285
TH $\alpha$	044-PSYLDKDEQCVVCGDKATGYHYRCITCEGCKGFFRRTIQLNLHPTSYCKY--DSCCVIDKITRNQCLCRFKKCIAVGM-120		P10827
TH $\beta$	098-PSYLDKDELCVVCGDKATGYHYRCITCEGCKGFFRRTIQLNLHPTSYCKY--EGKCVIDKTRRNQCRFHKCIYVGM-174		P10828
TR2	104-QGPNKVFDLCVVCGDKASGRHYGAVTCEGCKGFFKRSIRK--NLVYSCRG--SKDCIINKHHRNRCQYCRLLQRCIAFGM-178		P13056
TR4	108-VQRQPQVEYCVVCGDKASGRHYGAVSCEGCKGFFKRSVRK--NLTYSCRS--NQDCIINKHHRNRCQFCRLLKCKLEMGM-182		P49116
VDR	015-DFDRNVPRI $\text{CGV}$ CCDRATGFHFNAMTCEGCKGFFRSMKR--KALFTCPF--NGDCRITKDNRHRCQACRLRKCRVIGM-089		P11473
HNF4 $\alpha$	051-PNSLGVSAL $\text{CAI}$ CGDRATGKHYGASSCDGCKGFFRRSVRK--NHMYSCRF--SRQCVVDKDKRNQCRYCRLLRKCFRAGM-125		P41235
HNF4 $\beta$	003-TTDNGVNCL $\text{CAI}$ CGDRATGKHYGASSCDGCKGFFRRSIRK--SHVYSCRF--SRQCVVDKDKRNQCRYCRLLRKCFRAGM-077		Q14541
TLX	007-STSRILIDIPCKVCGDRSSGKHYGVYACDGCGSFFKRSIRR--NRTYVCKSGNQGGCPVDKTHRNQCRACRLKCKLEVNM-083		Q9Y466
PNR	037-PTGVSPSLQCRVCGDSSSGKHYGIYACNGCSGFFKRSVRR--RLIYRCQVG-AGMC PVDKAHRNQCRACRLKKCLQAGM-113		Q9Y5X4
AR	550-DYYFPQKTCIICGDEASGCHYGAUTCGSKVFFKRAAEG--KQKYICAS--RNDCTIDKFRRNCPSCRLRKCYEAGM-624		P10275
GR	412-ATTGPPPPLCLVCSDDEASGCHYGVLT $\text{CGSCKVFF}$ KRAVEG--QHNYICAG--RNDCIIDKIRRNCPACRYRKCLQAGM-486		P04150
MR	594-TGSSRPSKICLVCGDEASGCHYGVVT $\text{CGSCKVFF}$ KRAVEG--QHNYICAG--RNDCIIDKIRRNCPACRLQKCLQAGM-668		P08235
PR	558-SFESLPQKICIICGDEASGCHYGVLT $\text{CGSCKVFF}$ KRAMEG--QHNYICAG--RNDCIVDKIRRNCPACRLRKCCQAGM-632		P06401

FIGURE 8: Amino acid sequence alignment of DB domains of all known members of the human NR family. Absolutely conserved residues are colored red, while all other residues are colored black. Each member is denoted by its acronym in the left column, with the corresponding ExPasy code provided in the right column for access to the complete proteomic details of each member. The numerals hyphenated to the amino acid sequence at each end denote the boundaries of DB domains for each member. The cysteine residues within each of the two zinc fingers of DB domains, denoted ZF-I and ZF-II, that coordinate the  $Zn^{2+}$  ion in a tetrahedral arrangement are indicated by vertical arrows. Residues D190, H196, E203, and K206, located within the DB domain of ER $\alpha$ , are indicated by vertical arrows.

in hepatocyte nuclear factor 4a (HNF4a), hepatocyte nuclear factor 4g (HNF4g), and the tail-less orphan receptor (TLX), indicating that protonation at this position upon binding to DNA may also be critical for these nuclear receptors. Thus, the highly conserved nature of H196 and E203 among the functionally diverse members of the human NR family argues strongly that the proton-coupled binding to DNA may have evolved as a general mechanism for nuclear receptor function and regulation.

It is also worth noting that residue D190 is absolutely conserved among all members of the human NR family, implying

that although it does not serve as a proton acceptor, it must also play a pivotal role in protein–DNA interactions pertinent to nuclear receptors. Additionally, our thermodynamic data indicate that the D190A substitution has no bearable effect on the binding affinity of the DB domain of ER $\alpha$  for DNA (Table 2), an observation that is in conflict with evolutionary constraints being placed upon this residue in the human NR family. Further scrutiny of the binding of the wild-type DB domain (DB\_WT) versus the D190A mutant (DB\_D190A) to DNA suggests that although they bind with virtually indistinguishable affinities, the

underlying thermodynamic forces display distinct features. Thus, while the binding of both domains is driven by favorable enthalpic factors accompanied by entropic penalties, DB\_D190A generates twice as much heat relative to DB\_WT, implying that this residue may be critical for the folding and stability of ER $\alpha$  and that the more favorable heat likely results from the partial folding of the DB\_D190A mutant domain upon binding to DNA as noted earlier.

In an effort to further decipher the molecular basis of how nuclear receptors bind to their cognate DNA promoter elements with specificity, we also analyzed and compared the thermodynamics of binding of the ERE duplex to the DB domain of ER $\alpha$  containing alanine substitutions for a number of additional amino acid residues located at the protein–DNA interface (Table 2). These point mutations include S193A (DB\_S193A), Y197A (DB\_Y197A), S201A (DB\_S201A), K206A (DB\_K206A), K210A (DB\_K210A), and R211A (DB\_R211A). As shown in Table 2, alanine substitution of these residues weakens the binding of the DB domain to DNA by as little as 2-fold in the case of the S193A mutation and by as much as 17-fold in the case of the R211A mutation relative to the wild-type construct, implying that these residues contribute differentially to the free energy of binding. Of these six residues at the protein–DNA interface, only R211 is absolutely conserved within the DB domains of all nuclear receptors (Figure 8). This salient observation suggests strongly that in addition to H196 and E203, R211 is also likely to be a critical residue involved in the binding of all nuclear receptors to their cognate DNA sequences. However, the fact that residues S193, Y197, S201, K206, and K210 exhibit variability within the DB domains of nuclear receptors argues strongly in favor of their role in determining the specificity of binding of nuclear receptors to DNA. Nonetheless, it should be borne in mind that a complete understanding of the molecular basis of DNA specificity of nuclear receptors awaits detailed thermodynamic analysis coupled with site-directed mutagenesis of specific amino acid residues within DB domains of other nuclear receptors that we hope to accomplish in our future studies.

## CONCLUSIONS

Nuclear receptor function is tightly regulated by a multitude of post-translational modifications such as phosphorylation, acetylation, sumoylation, ubiquitination, and glycosylation (44–47). However, such modifications usually occur in regions outside the DB domain. The fact that the DB domain of ER $\alpha$  is directly regulated via the proton-coupled equilibrium of two critical residues, H196 and E203, located at the protein–DNA interface not only adds to the repertoire of tricks and treats employed by nuclear receptors but also has significant implications for improving our understanding of this important family of transcription factors.

Although the binding of the DB domain of ER $\alpha$  to DNA appears to be coupled to proton uptake, it is not clear from our data how such a coupled equilibrium might dictate the physiological role of this important nuclear receptor. Changes in intracellular pH regulate a multitude of cellular processes such as metabolic homeostasis and apoptosis (48). Furthermore, it is believed that ionizable residues within proteins sense such changes and activate a variety of proton pumps and ion transporters that in turn mediate extracellular transport of protons and anions to regulate intracellular pH (49–51). It is thus conceivable that changes in intracellular pH may also tightly regulate the transcriptional activity of ER $\alpha$  through direct

modulation of two ionizable residues, H196 and E203, located at the protein–DNA interface. Protonation of such residues would clearly enhance intermolecular hydrogen bonding and electrostatic interactions critical to driving this key protein–DNA interaction and vice versa. Although pK<sub>a</sub> values of side chains of histidine and glutamate within proteins are ~6 and ~4, respectively (52), these are likely to be influenced by the neighboring ionizable amino acid residues in the DB domain as noted earlier (Figure 1). Thus, protonation and deprotonation of H196 and E203 may not necessarily require large changes but may be mediated by small changes in intracellular pH. Whatever the exact physiological role of proton-coupled equilibrium observed here, this study clearly suggests further investigation of the role of pH in physiological processes governed by ER $\alpha$  and other nuclear receptors.

In the crystal structure of the DB domain of ER $\alpha$  in complex with the ERE duplex determined nearly two decades ago (28), it was proposed that the negative charge on E203 was largely neutralized through the formation of a salt bridge with the neighboring K206. On the other hand, our study here shows that the negative charge on E203 is rather neutralized through its protonation, allowing it to participate in the formation of hydrogen bonding with DNA in a more harmonious manner. Additionally, the crystal structural analysis also suggested the involvement of H196 in dictating protein–DNA interactions through hydrogen bonding with the phosphate backbone. The fact that H196 acquires a net positive charge through protonation upon the binding of DNA suggests that H196 is more likely to engage in the formation of a salt bridge with the phosphate backbone. Altogether, our study exquisitely reveals how a combined approach involving site-directed mutagenesis in conjunction with thermodynamics can complement structural data and further define key residues involved in protein–DNA interactions.

In short, this study demonstrates that the protonation of H196 and E203 in ER $\alpha$  is coupled to the binding of DNA and that such protonation is required for high-affinity protein–DNA interaction through thermodynamic optimization of intermolecular contacts. Given that H196 and E203 are conserved in a vast majority of ~50 members of the nuclear receptor family, our findings suggest that the nuclear receptors may act as sensors of intracellular pH and bear important consequences for a paradigm shift of their molecular action. Finally, the proton-coupled equilibrium characterized here may serve as a novel target for therapeutic intervention of nuclear receptors.

## ACKNOWLEDGMENT

We are deeply indebted to Thomas Harris, Marius Sudol, and Vineet Gupta for their critical reading of the manuscript and many helpful suggestions.

## REFERENCES

- Evans, R. M. (1988) The steroid and thyroid hormone receptor superfamily. *Science* 240, 889–895.
- Escriva, H., Bertrand, S., and Laudet, V. (2004) The evolution of the nuclear receptor superfamily. *Essays Biochem.* 40, 11–26.
- Thornton, J. W. (2001) Evolution of vertebrate steroid receptors from an ancestral estrogen receptor by ligand exploitation and serial genome expansions. *Proc. Natl. Acad. Sci. U.S.A.* 98, 5671–5676.
- McKenna, N. J., Cooney, A. J., DeMayo, F. J., Downes, M., Glass, C. K., Lanz, R. B., Lazar, M. A., Mangelsdorf, D. J., Moore, D. D., Qin, J., Steffen, D. L., Tsai, M. J., Tsai, S. Y., Yu, R., Margolis, R. N., Evans, R. M., and O'Malley, B. W. (2009) Minireview: Evolution of

- NURSA, the Nuclear Receptor Signaling Atlas. *Mol. Endocrinol.* 23, 740–746.
5. McEwan, I. J. (2009) Nuclear receptors: One big family. *Methods Mol. Biol.* 505, 3–18.
  6. Barnett, P., Tabak, H. F., and Hettema, E. H. (2000) Nuclear receptors arose from pre-existing protein modules during evolution. *Trends Biochem. Sci.* 25, 227–228.
  7. Kumar, R., and Thompson, E. B. (1999) The structure of the nuclear hormone receptors. *Steroids* 64, 310–319.
  8. Egea, P. F., Klaholz, B. P., and Moras, D. (2000) Ligand-protein interactions in nuclear receptors of hormones. *FEBS Lett.* 476, 62–67.
  9. Claessens, F., and Gewirth, D. T. (2004) DNA recognition by nuclear receptors. *Essays Biochem.* 40, 59–72.
  10. Green, S., and Chambon, P. (1988) Nuclear receptors enhance our understanding of transcription regulation. *Trends Genet.* 4, 309–314.
  11. Darimont, B. D., Wagner, R. L., Apriletti, J. W., Stallcup, M. R., Kushner, P. J., Baxter, J. D., Fletterick, R. J., and Yamamoto, K. R. (1998) Structure and specificity of nuclear receptor-coactivator interactions. *Genes Dev.* 12, 3343–3356.
  12. Ham, J., and Parker, M. G. (1989) Regulation of gene expression by nuclear hormone receptors. *Curr. Opin. Cell Biol.* 1, 503–511.
  13. Kato, S., Endoh, H., Masuhiro, Y., Kitamoto, T., Uchiyama, S., Sasaki, H., Masushige, S., Gotoh, Y., Nishida, E., Kawashima, H., Metzger, D., and Chambon, P. (1995) Activation of the estrogen receptor through phosphorylation by mitogen-activated protein kinase. *Science* 270, 1491–1494.
  14. Warnmark, A., Treuter, E., Wright, A. P., and Gustafsson, J. A. (2003) Activation functions 1 and 2 of nuclear receptors: Molecular strategies for transcriptional activation. *Mol. Endocrinol.* 17, 1901–1909.
  15. Noy, N. (2007) Ligand specificity of nuclear hormone receptors: Sifting through promiscuity. *Biochemistry* 46, 13461–13467.
  16. Gottlieb, B., Beitel, L. K., Wu, J., Elhaji, Y. A., and Trifiro, M. (2004) Nuclear receptors and disease: Androgen receptor. *Essays Biochem.* 40, 121–136.
  17. Gurnell, M., and Chatterjee, V. K. (2004) Nuclear receptors in disease: Thyroid receptor  $\beta$ , peroxisome-proliferator-activated receptor  $\gamma$  and orphan receptors. *Essays Biochem.* 40, 169–189.
  18. Brzozowski, A. M., Pike, A. C., Dauter, Z., Hubbard, R. E., Bonn, T., Engstrom, O., Ohman, L., Greene, G. L., Gustafsson, J. A., and Carlquist, M. (1997) Molecular basis of agonism and antagonism in the oestrogen receptor. *Nature* 389, 753–758.
  19. Sonoda, J., Pei, L., and Evans, R. M. (2008) Nuclear receptors: Decoding metabolic disease. *FEBS Lett.* 582, 2–9.
  20. Jensen, E. V., and Jacobson, H. (1962) Basic guides to the mechanism of estrogen action. *Recent Prog. Horm. Res.* 18, 318–414.
  21. Jensen, E. V. (1962) On the mechanism of estrogen action. *Perspect. Biol. Med.* 6, 47–59.
  22. Toft, D., and Gorski, J. (1966) A receptor molecule for estrogens: Isolation from the rat uterus and preliminary characterization. *Proc. Natl. Acad. Sci. U.S.A.* 55, 1574–1581.
  23. Toft, D., Shyamala, G., and Gorski, J. (1967) A receptor molecule for estrogens: Studies using a cell-free system. *Proc. Natl. Acad. Sci. U.S.A.* 57, 1740–1743.
  24. Jensen, E. V., and Jordan, V. C. (2003) The estrogen receptor: A model for molecular medicine. *Clin. Cancer Res.* 9, 1980–1989.
  25. Heldring, N., Pike, A., Andersson, S., Matthews, J., Cheng, G., Hartman, J., Tujague, M., Strom, A., Treuter, E., Warner, M., and Gustafsson, J. A. (2007) Estrogen receptors: How do they signal and what are their targets. *Physiol. Rev.* 87, 905–931.
  26. Kumar, V., Green, S., Stack, G., Berry, M., Jin, J. R., and Chambon, P. (1987) Functional domains of the human estrogen receptor. *Cell* 51, 941–951.
  27. Klinge, C. M. (2001) Estrogen receptor interaction with estrogen response elements. *Nucleic Acids Res.* 29, 2905–2919.
  28. Schwabe, J. W., Chapman, L., Finch, J. T., and Rhodes, D. (1993) The crystal structure of the estrogen receptor DNA-binding domain bound to DNA: How receptors discriminate between their response elements. *Cell* 75, 567–578.
  29. Schwabe, J. W., Neuhaus, D., and Rhodes, D. (1990) Solution structure of the DNA-binding domain of the oestrogen receptor. *Nature* 348, 458–461.
  30. Gasteiger, E., Hoogland, C., Gattiker, A., Duvaud, S., Wilkins, M. R., Appel, R. D., and Bairoch, A. (2005) In The Proteomics Protocols Handbook (Walker, J. M., Ed.) pp 571–607, Humana Press, Totowa, NJ.
  31. Cantor, C. R., Warshaw, M. M., and Shapiro, H. (1970) Oligonucleotide interactions. 3. Circular dichroism studies of the conformation of deoxyoligonucleotides. *Biopolymers* 9, 1059–1077.
  32. Wiseman, T., Williston, S., Brandts, J. F., and Lin, L. N. (1989) Rapid measurement of binding constants and heats of binding using a new titration calorimeter. *Anal. Biochem.* 179, 131–137.
  33. Fukada, H., and Takahashi, K. (1998) Enthalpy and heat capacity changes for the proton dissociation of various buffer components in 0.1 M potassium chloride. *Proteins* 33, 159–166.
  34. Kozlov, A. G., and Lohman, T. M. (2000) Large contributions of coupled protonation equilibria to the observed enthalpy and heat capacity changes for ssDNA binding to *Escherichia coli* SSB protein. *Proteins* 4 (Suppl.), 8–22.
  35. Ortiz-Salmeron, E., Yassin, Z., Clemente-Jimenez, M. J., Las Heras-Vazquez, F. J., Rodriguez-Vico, F., Baron, C., and Garcia-Fuentes, L. (2001) Thermodynamic analysis of the binding of glutathione to glutathione S-transferase over a range of temperatures. *Eur. J. Biochem.* 268, 4307–4314.
  36. Marti-Renom, M. A., Stuart, A. C., Fiser, A., Sanchez, R., Melo, F., and Sali, A. (2000) Comparative Protein Structure Modeling of Genes and Genomes. *Annu. Rev. Biophys. Biomol. Struct.* 29, 291–325.
  37. Carson, M. (1991) Ribbons 2.0. *J. Appl. Crystallogr.* 24, 958–961.
  38. Koradi, R., Billeter, M., and Wuthrich, K. (1996) MOLMOL: A program for display and analysis of macromolecular structures. *J. Mol. Graphics* 14, 51–55.
  39. Lumry, R., and Rajender, S. (1970) Enthalpy-entropy compensation phenomena in water solutions of proteins and small molecules: A ubiquitous property of water. *Biopolymers* 9, 1125–1227.
  40. Eftink, M. R., Anusiem, A. C., and Biltonen, R. L. (1983) Enthalpy-entropy compensation and heat capacity changes for protein-ligand interactions: General thermodynamic models and data for the binding of nucleotides to ribonuclease A. *Biochemistry* 22, 3884–3896.
  41. Cooper, A., Johnson, C. M., Lakey, J. H., and Nollmann, M. (2001) Heat does not come in different colours: Entropy-enthalpy compensation, free energy windows, quantum confinement, pressure perturbation calorimetry, solvation and the multiple causes of heat capacity effects in biomolecular interactions. *Biophys. Chem.* 93, 215–230.
  42. Sharp, K. (2001) Entropy-enthalpy compensation: Fact or artifact? *Protein Sci.* 10, 661–667.
  43. Starikov, E. B., and Norden, B. (2007) Enthalpy-entropy compensation: A phantom or something useful? *J. Phys. Chem. B* 111, 14431–14435.
  44. Chen, Y. X., Du, J. T., Zhou, L. X., Liu, X. H., Zhao, Y. F., Nakanishi, H., and Li, Y. M. (2006) Alternative O-GlcNAcylation/O-phosphorylation of Ser16 induce different conformational disturbances to the N terminus of murine estrogen receptor  $\beta$ . *Chem. Biol.* 13, 937–944.
  45. Faus, H., and Haendler, B. (2006) Post-translational modifications of steroid receptors. *Biomed. Pharmacother.* 60, 520–528.
  46. Popov, V. M., Wang, C., Shirley, L. A., Rosenberg, A., Li, S., Nevalainen, M., Fu, M., and Pestell, R. G. (2007) The functional significance of nuclear receptor acetylation. *Steroids* 72, 221–230.
  47. Weigel, N. L., and Moore, N. L. (2007) Steroid receptor phosphorylation: A key modulator of multiple receptor functions. *Mol. Endocrinol.* 21, 2311–2319.
  48. Boron, W. F. (2004) Regulation of intracellular pH. *Adv. Physiol. Educ.* 28, 160–179.
  49. Khaled, A. R., Moor, A. N., Li, A., Kim, K., Ferris, D. K., Muegge, K., Fisher, R. J., Fliegel, L., and Durum, S. K. (2001) Trophic factor withdrawal: p38 mitogen-activated protein kinase activates NHE1, which induces intracellular alkalinization. *Mol. Cell. Biol.* 21, 7545–7557.
  50. Khaled, A. R., Reynolds, D. A., Young, H. A., Thompson, C. B., Muegge, K., and Durum, S. K. (2001) Interleukin-3 withdrawal induces an early increase in mitochondrial membrane potential unrelated to the Bcl-2 family. Roles of intracellular pH, ADP transport, and  $F_0F_1$ -ATPase. *J. Biol. Chem.* 276, 6453–6462.
  51. Puceat, M., Roche, S., and Vassort, G. (1998) Src family tyrosine kinase regulates intracellular pH in cardiomyocytes. *J. Cell Biol.* 141, 1637–1646.
  52. Harris, T. K., and Turner, G. J. (2002) Structural basis of perturbed pKa values of catalytic groups in enzyme active sites. *IUBMB Life* 53, 85–98.